/EtOAc, 3:2). Compound *altro*-**9b** (60 mg, 24%) (the ^{1}H NMR spectrum was identical with that of an authentic sample) was eluted first from the column, followed by **18b** (66 mg, 25%) (the ^{1}H NMR spectrum of this sample was identical with that for **18b** prepared above).

1-(3-Cyanopyridin-5-yl)-2,3:4,5-di-*O*-isopropylidene-1-keto-D-*ribo*-pent-1-ulose (19a). To a mixture of CrO_3 (300 mg), pyridine 0.5 mL), and Ac_2O (0.3 mL) in CH_2Cl_2 (7 mL) was added *altro*-**9a** (334 mg, 1 mmol), and the mixture was stirred at room temperature for 1 h. The mixture was diluted with EtOAc (50 mL) and filtered through a silica gel pad from an insoluble solid. The solid was washed with EtOAc (50 mL). The combined organic solutions were concentrated in vacuo, and the residue was crystallized from EtOH to give **19a** (293 mg, 88%): mp 155-156 °C; ^{1}H NMR ($CDCl_3$) δ 1.05 (6 H, s, *i*-Pr), 1.45 (3 H, s, *i*-Pr), 1.60 (3 H, s, *i*-Pr), 3.87-4.07 (3 H, m, H-4',5',5''), 4.40 (1 H, dd, H-3', $J_{3',4'}$ = 2.7 Hz, $J_{2',3'}$ = 6.3 Hz), 5.49 (1 H, d, H-2'), 8.50 (1 H, t, H-4, $J_{2,4} = J_{4,6}$ = 2.2 Hz), 9.01 (1 H, d, H-6), 9.30 (1 H, d, H-2). Anal. Calcd for $C_{17}H_{20}N_2O_5$: C, 61.43; H, 6.07; N, 8.42. Found: C, 61.31; H, 6.06; N, 8.35.

In a similar manner, *altro*-**9b** (388 mg, 1.0 mmol) was oxidized to **1-(2-bromopyridin-6-yl)-2,3:4,5-di-*O*-isopropylidene-1-keto-D-*ribo*-pent-1-ulose (19b)** as a foam: ^{1}H NMR ($CDCl_3$) δ 0.77 (3 H, s, *i*-Pr), 1.00 (3 H, s, *i*-Pr), 1.46 (3 H, s, *i*-Pr), 1.57 (3 H, s, *i*-Pr), 3.91-4.10 (3 H, m, H-4',5',5''), 4.51-4.80 (1 H, m, H-3'), 6.00 (1 H, d, H-2', $J_{2',3'}$ = 5.7 Hz), 7.26-7.91 (2 H, m, H-3,5), 8.00 (1 H, dd, H-4, $J_{3,4}$ = 2.7 Hz, $J_{4,5}$ = 6.0 Hz). Anal. Calcd for $C_{16}H_{20}BrNO_5$: C, 49.75; H, 5.22; N, 3.63. Found: C, 49.69; H, 5.43; N, 3.60.

Reduction of 19a. Synthesis of *allo*-9a. To a solution of **19a** (100 mg, 0.3 mmol) in EtOH (10 mL) was added $NaBH_4$ (445 mg, 116 mmol), and the mixture was stirred at room temperature for 2 h. The mixture was diluted with MeOH (4 mL) and concentrated in vacuo, and the residue was flash chromatographed on a silica gel column (1% EtOH in $CHCl_3$, v/v) to give *allo*-**9a** (80 mg, 79%). The ^{1}H NMR spectrum of this sample was identical with that of *allo*-**9a** prepared before.

In a similar manner, **9b** (110 mg, 0.29 mmol) was reduced with $NaBH_4$ (43 mg, 1.13 mmol) to give *allo*-**9b** (79 mg, 72%).

Acknowledgment. We thank Dr. F. H. Field of the Mass Spectrometric Biotechnology Research Resource, Rockefeller University, for the mass spectrometry data. We also thank Anna Ptak for her excellent technical assistance. This investigation was supported in part by funds from the National Cancer Institute, National Institutes of Health USDHHS (Grants No. CA-08749 and CA-33907).

On the Origin of Cavity-Filling Conformations of Macrocycles: A ^{1}H NMR Spectroscopic and Force-Field Computational Study

Richard J. Loncharich, Eileen Seward, Stephen B. Ferguson, Frank K. Brown, François Diederich,* and K. N. Houk*

Department of Chemistry and Biochemistry, University of California, Los Angeles, Los Angeles, California 90024-1569

Received January 19, 1988

Recently reported ^{1}H NMR studies indicated that the phenanthrene macrocycle **2** preferred a conformation with the phenanthrene unit turned inside the intramolecular cavity formed by the diphenylmethane unit and the two alkyl side chains. The preference of this cavity-filling conformation was supported by molecular mechanics force-field calculations of a few arbitrary conformations of the macrocycle **2**. Force-field calculations were also performed on the closely related biphenyl macrocycle **3** and suggested different conformation characteristics of the biphenyl unit. These computational predictions initiated the synthesis of **3** and the analysis of macrocycles **2** and **3** by 1D NOE and 2D NOESY and COSY ^{1}H NMR spectroscopic methods. These experimental studies support a conformation in which the phenanthrene unit is embedded deeply inside the cavity of macrocycle **2**. The studies also indicate that the conformational behavior of the biphenyl macrocycle **3** consists of conformations that have one phenyl ring folded into the cavity in dynamic equilibrium with conformations consisting of the biphenyl unit outside the cavity. In addition, a more rigorous conformational analysis using the ELLIPSE algorithm to generate initial conformations, AMBER and MM2 force-field calculations to minimize conformations, and molecular dynamics simulations was performed to understand better the origin of cavity-filling conformations and the differences in conformational behavior between **2** and **3**. These computational studies indicate that the cavity-filling conformation of macrocycle **2** is favored by 4-6 kcal/mol, while the conformations of macrocycle **3** with the biphenyl inside the cavity or with one phenyl ring inside the cavity are the favored conformations.

Introduction

In a series of systematic studies, Cram et al. have demonstrated elegantly the importance of host preorganization for the strength of host-guest interactions.[1] For complexes exhibiting similar stereoelectronic complementarity between the molecular binding site and the guest, the degree of preorganization largely determines the amount of free energy gained by complexation in a specific solvent. If a section of the host can block or close off the binding cavity, some of the energy gained in the complexation process will be needed for the reorganization of the binding site, thus reducing the complexation capabilities of the host. The extraordinarily strong binding of cations by spherands[2] and the strong binding of neutral arenes in aqueous and organic solvents by a macrobicyclic cyclophane host[3] illustrates the significance of enforced, preorganized binding sites for efficient host-guest interactions.[4]

(1) Cram, D. J. *Angew. Chem.* **1986**, *98*, 1041-1060; *Angew. Chem., Int. Ed. Engl.* **1986**, *25*, 1039-1057.

(2) (a) Cram, D. J.; Kaneda, T.; Helgeson, R. C.; Brown, S. B.; Knobler, C. B.; Maverick, E.; Trueblood, K. N. *J. Am. Chem. Soc.* **1985**, *107*, 3645-3657. (b) Cram, D. J.; Lein, G. M. *J. Am. Chem. Soc.* **1985**, *107*, 3657-3668.

(3) Diederich, F.; Dick, K.; Griebel, D. *J. Am. Chem. Soc.* **1986**, *108*, 2273-2286.

(4) For other fully preorganized synthetic ligands, see: (a) Rebek, J., Jr. *Science (Washington, D.C.)* **1987**, *235*, 1478-1484. (b) Canceill, J.; Lacombe, L.; Collet, A. *J. Am. Chem. Soc.* **1986**, *108*, 4230-4232. (c) Mock, W. L.; Shih, N.-Y. *J. Org. Chem.* **1986**, *51*, 4440-4446. (d) Bell, T. W.; Firestone, A. *J. Am. Chem. Soc.* **1986**, *108*, 8109-8111. (e) Sheridan, R. E.; Whitlock, H. W., Jr. *J. Am. Chem. Soc.* **1986**, *108*, 7120-7121.

0022-3263/88/1953-3479$01.50/0

When macrocyclic cavities are constructed from a number of flexible units, part of the host molecule may fold into itself. If such cavity-filling conformations are quite stable, then the molecule may prove to be quite inhospitable. It is not always possible to predict by using CPK models the importance of cavity-filling conformations of a macrocyclic host. A better understanding of the interactions that favor cavity-filling conformations of macrocycles is required to avoid the construction of binding sites that require extensive reorganization during complexation and to enhance the probability of forming stable complexes.

Examples of designed hosts with segments that fold into a cavity have been shown by X-ray crystallographic analysis of free crown ethers[5] and cryptands.[6] In the field of cyclophane hosts with apolar binding sites, Mak et al. have shown that two of the benzene rings of crystalline 2,11,20,29-tetrathia[3.3.3.3]parabenzenophane effectively fill the central cavity.[7] Tabushi et al. had previously demonstrated that the peralkylated tetrasulfonium salt of this macrocycle will still form a complex with 8-(phenylamino)-1-naphthalenesulfonate in aqueous solution.[8] X-ray crystal structures of larger calix[n]arenes ($n \geq 6$) reveal that the macrocyclic cavities are filled by groups of these compounds.[9]

The conformation observed in crystal structures, however, can be influenced to a large extent by the tendency to maximize the crystal density and to minimize the molecular volume. Such conformations do not necessarily reflect the conformations of free macrocycles in solution. In solution, ^{1}H NMR spectroscopic evidence for cavity-filling conformations of free macrocycles was obtained for polypyridino-crowns[10] and for a polytopic receptor consisting of two diaza-crowns bridged by a porphyrin and a biphenyl unit.[11] ^{13}C NMR longitudinal relaxation time measurements showed that the aromatic rings of suitably sized 2,6-pyrido- and benzo-crown ethers can fill the macrocyclic cavities in solution.[12] Cavity-filling conformations of the latter macrocycles could also be located by molecular mechanics calculations.

In an attempt to synthesize chiral host 1 designed to complex apolar neutral guests,[13] Diederich et al. prepared the phenanthrene macrocycle **2**.[14] Ozonolysis of the reactive 9,10-bond of phenanthrenes normally proceeds smoothly and in very high yield.[15] This reaction was therefore the method of choice for transforming the phenanthrene macrocycle **2** to a precursor of 1 incorporating a 2,2′,6,6′-tetrasubstituted biphenyl unit. The ozonation of the 9,10-bond of the phenanthrene moiety of **2**, however, was unsuccessful under all applied experimental conditions. A preliminary ^{1}H NMR analysis[14] indicated that the phenanthrene unit does not take the orientation shown by **2** but is preferentially turned into the intramolecular cavity formed by the diphenylmethane unit and the two alkyl chains as shown schematically by **2a**. The reactive 9,10-bond of the phenanthrene moiety is therefore efficiently shielded from attack by ozone. Hence the reaction of ozone at the electron-rich aromatic rings of the diphenylmethane unit, at other positions of the phenanthrene moiety, and at the benzylic ether groups[16] becomes competitive. This explains the large number of products formed in the ozonation of **2**.

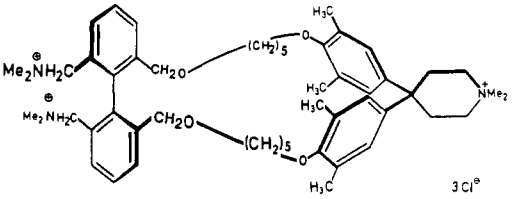

1

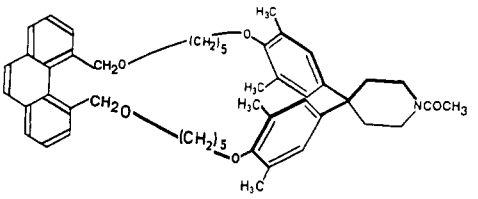

2

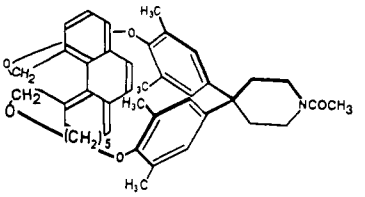

2a

In this paper, 1D NOE and 2D NOESY ^{1}H NMR evidence supports the exclusive presence of cavity-filling conformations similar to **2a** in solution. Indeed preliminary force-field calculations using MM2[17] showed that geometries such as **2a** represent low energy conformations of **2**. In addition, these preliminary calculations predicted that the new biphenyl macrocycle **3** would differ in its conformational characteristics from the closely related phenanthrene macrocycle **2**. This prediction initiated the synthesis of **3** and 1D and 2D ^{1}H NMR studies of this macrocycle are described below. These studies support the predicted differences in the conformational behavior of **2** and **3** in solution. A thorough conformational analysis using both the AMBER[18] and the MM2 force fields and

(5) (a) Maverick, E.; Seiler, P.; Schweizer, W. B.; Dunitz, J. D. *Acta. Crystallogr. Sect. B* **1980**, *36*, 615–620. (b) Newkome, G. R.; Majestic, V. K.; Fronczek, F. R. *Tetrahedron Lett.* **1981**, *22*, 3035–3038. (c) Uiterwijk, J. W. H. M.; van Staveren, C. J.; Reinhoudt, D. N.; den Hertog, H. J., Jr.; Kruise, L.; Harkema, S. *J. Org. Chem.* **1986**, *51*, 1575–1587. (d) Slawin, A. M. Z.; Spencer, N.; Stoddart, J. F.; Williams, D. J. *J. Chem. Soc., Chem. Commun.* **1987**, 1070–1072.

(6) (a) Metz, B.; Moras, D.; Weiss, R. *J. Chem. Soc., Perkin Trans. 2* **1976**, 423–429. (b) Pascard, C.; Riche, C.; Cesario, M.; Kotzyba-Hibert, F.; Lehn, J.-M. *J. Chem. Soc., Chem. Commun.* **1982**, 557–559. (c) Vögtle, F.; Müller, W. M.; Puff, H.; Friedrichs, E. *Chem. Ber.* **1983**, *116*, 2344–2354.

(7) Chan, T.-L.; Mak, T. C. W. *Acta Crystallogr. Sect. C* **1984**, *40*, 1452–1454.

(8) Tabushi, I.; Sasaki, H.; Kuroda, Y. *J. Am. Chem. Soc.* **1976**, *98*, 5727–5728.

(9) (a) Andreetti, G. D.; Ungaro, R.; Pochini, A. *J. Chem. Soc., Chem. Commun.* **1981**, 533–534. (b) Ungaro, R.; Pochini, A.; Andreetti, G. D.; Domiano, P. *J. Incl. Phenom.* **1985**, *3*, 35–42.

(10) Newkome, G. R.; Hager, D. C.; Kiefer, G. E. *J. Org. Chem.* **1986**, *51*, 850–853.

(11) Hamilton, A.; Lehn, J.-M.; Sessler, J. L. *J. Am. Chem. Soc.* **1986**, *108*, 5158–5167.

(12) Grootenhuis, P. D. J.; van Eerden, J.; Sudhölter, E. J. R.; Reinhoudt, D. N.; Roos, A.; Harkema, S.; Feil, D. *J. Am. Chem. Soc.* **1987**, *109*, 4792–4797.

(13) (a) Diederich, F. *Angew. Chem.* **1988**, *100*, 372–396; *Angew. Chem. Int. Ed. Engl.* **1988**, *27*, 362–386. (b) Dharanipragada, R.; Diederich, F. *Tetrahedron Lett.* **1987**, *28*, 2443–2446. (c) Dharanipragada, R.; Ferguson, S. B.; Diederich, F. *J. Am. Chem. Soc.* **1988**, *110*, 1679–1690. (d) Diederich, F.; Dick, K.; Griebel, D. *Chem. Ber.* **1985**, *118*, 3588–3619.

(14) Rubin, Y.; Dick, K.; Diederich, F.; Georgiadis, T. M. *J. Org. Chem.* **1986**, *51*, 3270–3278.

(15) Bailey, P. S. *Ozonation in Organic Chemistry*; Academic: New York, 1982; Vol. II, pp 60–72.

(16) Reference 15, pp 285–295.

(17) (a) Burkert, U.; Allinger, N. L. *Molecular Mechanics*; American Chemical Society: Washington, DC, 1982. (b) Allinger, N. L. *J. Am. Chem. Soc.* **1977**, *99*, 8127–8134. (c) Allinger, N. L.; Yuh, Y. H. *Molecular Mechanics II*, QCPE No 395, Indiana University, Bloomington, IN.

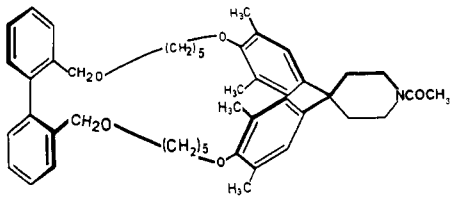

3

including molecular dynamics was then undertaken to understand the origin of cavity-filling conformations and the differences in conformational characteristics between **2** and **3**. In this analysis, described below, a comparison of the low energy conformations generated by the two force fields for the two large 29-membered macrocycles is made. Such a comparison has not been made in previous conformational analyses of macrocyclic hosts and their complexes that utilized either one of the two force fields.[12,13c,19-21]

Synthesis of the Biphenyl Macrocycle 3. The synthesis of **3** was initially attempted by cyclizing 2,2′-bis(hydroxymethyl)biphenyl (**4**)[22] with 1-acetyl-4,4-bis[4-(5-chloropentoxy)-3,5-dimethylphenyl]piperidine (**7**)[14] in the presence of base. However, this reaction in tetrahydrofuran at various temperatures with sodium or potassium hydride as base and in the presence or absence of 18-crown-6 led mainly to oligomeric material.[14] The ^{1}H NMR spectra of the reaction mixtures showed the formation of a large amount of elimination products. The biphenyl macrocycle **3** finally was obtained in 21% from the cyclization of diphenol **6**[13d] with 2,2-bis[(5-chloropentoxy)-methyl]biphenyl (**5**) using cesium carbonate as base in dimethylformamide. The dichloride **5** was prepared in 71% yield in the reaction of **4** with a large excess of 1,5-dichloropentane in tetrahydrofuran (KH; 18-crown-6).

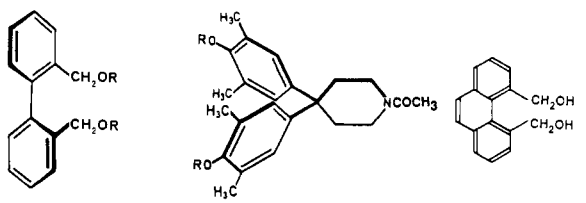

4 R = H
5 R = $(CH_2)_5$-Cl

6 R = H
7 R = Cl-$(CH_2)_5$

8

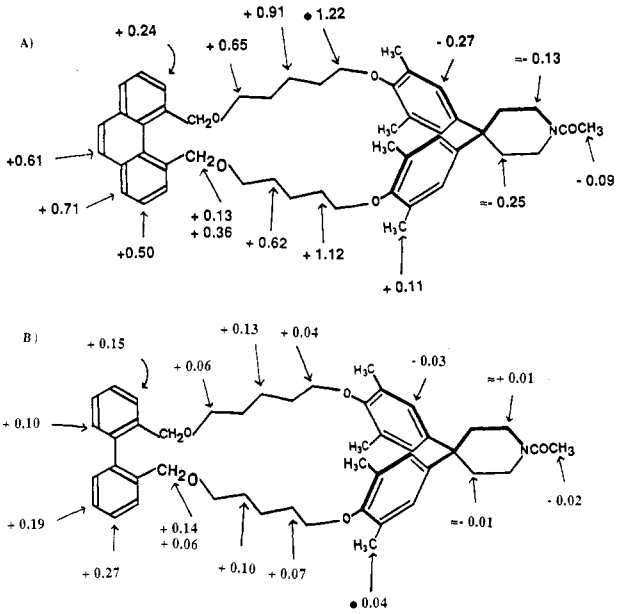

Figure 1. (A) Differences between the chemical shifts ($\Delta\delta$, + = upfield shift) of comparable protons of **2** and of the cyclization precursor **7**/**8** in $CDCl_3$. (B) Differences between the chemical shifts ($\Delta\delta$, + = upfield shift) of comparable protons of **3** and of the cyclization precursor **5**/**7** in $CDCl_3$. Multiplet centers are used to calculate the $\Delta\delta$ values. The δ values of **3** and **5**, needed to calculate $\Delta\delta$ values, are given in the Experimental Section, those of **2**, **7**, and **8** are given in ref 14.

^{1}H NMR Study of the Geometry of the Phenanthrene Macrocycle 2 in Solution. The comparison of the 360-MHz ^{1}H NMR spectra (1D and, for signal assignments, 2D COSY,[23] 303 K, $CDCl_3$) of **2** with the spectra of the cyclization precursors **7** and **8** provided strong evidence that the macrocycle prefers a cavity-filling conformation such as **2a**. Figure 1A shows the differences between the chemical shifts ($\Delta\delta$, + = upfield shift) of comparable protons of **2** and of the cyclization components **7** and **8** which can only be explained by preferred cavity-filling conformations as shown in **2a**.[14]

The changes in chemical shift shown in Figure 1A closely resemble the complexation shifts that are observed upon formation of highly structured complexes between diphenylmethane hosts and aromatic guests, e.g., pyrene in aqueous and organic solvents.[13,24] In these complexes, the aromatic guests assume a location very similar to the phenanthrene unit in **2a**. Therefore, the phenanthrene macrocycle **2** can be regarded as an interesting intramolecular model for these intermolecular complexes, and this aspect adds further interest to the detailed force-field analysis of **2** described below.

The differences between the chemical shifts of the protons of **2** and the chemical shifts of the cyclization precursors **7**/**8**, $\Delta\delta$, are almost identical in various solvents ($CDCl_3$, MeOH-d_4, Me_2SO-d_6) as well as over the temperature range of 200–400 K. It can therefore be concluded that cavity-filling conformations of **2** (e.g. **2a**) are considerably more stable than conformations with the phenanthrene moiety turned outwards. The ^{1}H NMR spectra also show that the geometry of **2** in methanol (c 5 × 10^{-3}

(18) (a) Weiner, P. K.; Kollman, P. A. *J. Comput. Chem.* **1981**, *2*, 287–303. (b) Weiner, S. J.; Kollman, P. A.; Case, D. A.; Singh, U. C.; Ghio, C.; Alagona, G.; Profeta, S., Jr.; Weiner, P. *J. Am. Chem. Soc.* **1984**, *106*, 765–784.

(19) For AMBER studies of cation-complexing ligands, see: (a) Wipff, G.; Weiner, P.; Kollman, P. *J. Am. Chem. Soc.* **1982**, *104*, 3249–3258. (b) Wipff, G.; Kollman, P. A. *Nouv. J. Chim.* **1985**, *9*, 457–465. (c) Kollman, P. A.; Wipff, G.; Singh, U. C. *J. Am. Chem. Soc.* **1985**, *107*, 2212–2219. (d) Venanzi, C. A.; Bunce, J. D. *Int. J. Quantum Chem., Quantum Biol. Symp.* **1986**, *12*, 69–87.

(20) For MM2 studies of cation-complexing ligands, see: (a) Bovill, M. J.; Chadwick, D. J.; Sutherland, I. O.; Watkin, D. *J. Chem. Soc., Perkin Trans. 2* **1980**, 1529–1543. (b) Perrin, R.; Decoret, C.; Bertholon, G.; Lamartine, R. *Nouv. J. Chim.* **1983**, *7*, 263–268. (c) Thõm, V. J.; Fox, C. C.; Boeyens, J. C. A.; Hancock, R. D. *J. Am. Chem. Soc.* **1984**, *106*, 5947–5955. (d) Dobler, M. *Chimia* **1984**, *38*, 415–421. (e) Drew, M. G. B.; Nicholson, D. G. *J. Chem. Soc., Dalton Trans.* **1986**, 1543–1549. (f) Geue, R.; Jacobson, S. H.; Pizer, R. *J. Am. Chem. Soc.* **1986**, *108*, 1150–1155. (g) Uiterwijk, J. W. H. M.; Harkema, S.; Feil, D. *J. Chem. Soc., Perkin Trans. 2* **1987**, 721–731.

(21) For the application of molecular mechanics to large cyclophanes and cyclophane-hosts, see: (a) Miller, S. P.; Whitlock, H. W. *J. Am. Chem. Soc.* **1984**, *106*, 1492–1494. (b) Whitlock, B. J.; Whitlock, H. W., Jr. *J. Am. Chem. Soc.* **1985**, *107*, 1325–1329. (c) Masek, B. B.; Santarsiero, B. D.; Dougherty, D. A. *J. Am. Chem. Soc.* **1987**, *109*, 4373–4379.

(22) Hall, D. M.; Lesslie, M. S.; Turner, E. E. *J. Chem. Soc.* **1950**, 711–713.

(23) (a) Rahman, A. u. *Nuclear Magnetic Resonance*, Springer: New York, 1986; Chapter 5, pp 202–313 and references cited therein. (b) Wüthrich, K. *NMR of Proteins and Nucleic Acids*; Wiley-Interscience: New York, 1986.

(24) (a) Diederich, F.; Dick, K. *J. Am. Chem. Soc.* **1984**, *106*, 8024–8036. (b) Diederich, F.; Griebel, D. *J. Am. Chem. Soc.* **1984**, *106*, 8037–8046.

mol·L^{-1}) is not changed if pyrene or phenanthrene is added to give a 0.05 M solution.

Homonuclear 2D nuclear Overhauser enhancement spectroscopy (NOESY)[23] provided additional evidence that the phenanthrene unit of **2** is located in close spatial proximity to the diphenylmethane unit. In the contour plot of the 2D chemical shift correlated ^{1}H NMR spectra of **2** (500 MHz, $CDCl_3$, T = 303 K) dipolar coupling through-space is observed between selected protons of the phenanthrene moiety and the diphenylmethane unit. Cross peaks clearly establish spatial interactions between the protons of the methyl groups of the diphenylmethane unit and the protons 9,10-H,[25] 1,8-H, and 2,7-H of the phenanthrene unit. The geometry, which is schematically depicted by **2a**, is further supported by the lack of observed connectivity between the methyl protons and the protons 3,6-H of the phenanthrene moiety. In the aromatic region, cross peaks connect the aromatic protons of the diphenylmethane unit at 7.09 and the protons 9,10-H of the phenanthrene unit at 6.97. Other cross peaks in the aromatic part of the spectrum appear in crowded regions which makes their assignment difficult.

The spatial proximity between the diphenylmethane and the phenanthrene units was further supported by 1D NOE difference spectroscopy (200 MHz, T = 303 K, $CDCl_3$, Ar).[26] Irradiation of the diphenylmethane methyl protons led to a 3% enhancement of the singlet for the phenanthrene protons 9,10-H.

In conclusion, the ^{1}H NMR studies and the results of the ozonation reaction strongly support a preferred geometry of **2** with the phenanthrene unit located deep in the macrocyclic cavity.

^{1}H NMR Study of the Geometry of the Biphenyl Macrocycle 3 in Solution. The ^{1}H NMR spectra of **3**, like those of **2**, do not show a significant dependency on solvent ($CDCl_3$, methanol-d_4, Me_2SO-d_6) or on temperature (200–400 K). When the proton chemical shifts of **3** are compared to those of the precursor molecules **5** and **7**, cyclization shifts ($\Delta\delta$) can be calculated that are shown in Figure 1B. All signals of **3** and the precursor molecules could be easily assigned with the help of 2D COSY spectra. The $\Delta\delta$ values of Figure 1B are less dramatic and less specific than those observed for the phenanthrene macrocycle **2** (Figure 1A). A special, cavity-filling conformation of macrocycle **3** does not seem predominant in solution.

It is difficult to relate the cyclization shifts ($\Delta\delta$) observed for **3** to specific macrocyclic geometries, since small torsional angle changes of the biphenyl unit can induce large chemical shift changes. It is only by comparing the $\Delta\delta$ values for **3** with the cyclization shifts for the previously prepared macrocycle **9**[14] that some structural information could be obtained. With its bulky amide substituents, the

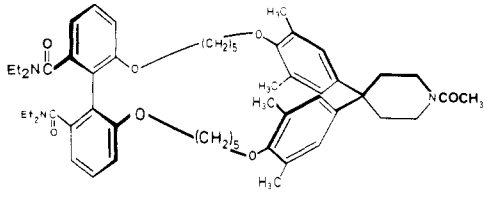

9

biphenyl unit of **9** cannot fold into the intramolecular cavity.[13c] The cyclization shifts observed for both macrocycles **3** and **9** are very similar except for the protons of the biphenyl unit. For the biphenyl unit of **9**, cyclization shifts of +0.15 (3,3′-H),[25] +0.10 (4,4′-H), and +0.02 (5,5′-H) are calculated. The diethylamide protons of **9** do not exhibit any cyclization shifts. The cyclization shifts of the biphenyl protons of **3** differ considerably from those of **9**, and the largest $\Delta\delta$ value is observed for 4,4′-H (+0.27) followed by 5,5′-H (+0.19) and by 3,3′-H (+0.15). These specific upfield shifts indicate that one of the phenyl rings of the biphenyl unit turns into the intramolecular cavity and points with its C-3–C-4–C-5 edge into the anisotropic shielding region of the diphenylmethane unit. The moderate upfield shifts show, however, that these partially cavity-filling conformations must be in a dynamic equilibrium with conformations which locate the biphenyl unit outside the cavity at a larger distance from the diphenylmethane unit.

Conformations with the biphenyl benzene rings in spatial proximity to the diphenylmethane unit are also supported by the observed dipolar through-space coupling. In the 2D NOESY spectrum (500 MHz, 293 K), cross signals connect the biphenyl protons 4,4′-H and 5,5′-H with the aromatic as well as with the methyl protons of the diphenylmethane unit. A weak signal enhancement (≤1%) for the biphenyl protons 4,4′-H and 5,5′-H is observed in the 1D NOE difference spectra (500 MHz, 293 K) upon irradiation of the diphenylmethane methyl protons.

In summary, the biphenyl macrocycle **3** shows a different conformational behavior than the phenanthrene macrocycle **2**. Conformations in which the biphenyl unit of **3**, like the phenanthrene unit of **2**, is deeply located in the binding site are not supported by the ^{1}H NMR data. The data suggest a dynamic equilibrium consisting of conformations with the biphenyl unit outside the cavity and conformations with one phenyl ring folding into the cavity.

Computational Methods. We undertook a computational study of these molecules to investigate why the phenanthrene macrocycle **2** adopts this unusual cavity-filling conformation and to predict the preferred conformation of related molecules such as macrocycle **3**. Since the prediction of conformations of molecules of this type had not previously been achieved, we also went to some lengths to evaluate several computational techniques to make such predictions. The AMBER (Kollman et al.)[18] and MM2 (Allinger)[17] empirical force fields have been used in this study. The AMBER program[18] includes convenient routines for the generation of macrocyclic structures and has molecular dynamics routines for simulating interconversions of conformations. AMBER has been devised mainly for the study of nucleic acids and proteins[18] but has also been used to investigate the conformations of such compounds as crown ethers[19] and spherands.[19c,d] The MM2 force field[17] has been used widely for conformational studies of large ring systems,[17a,27] cyclophanes, and cyclophane hosts,[21] and cryptands.[20f] The additional parameters which are not present in the standard parameter sets of the two force fields and had to be developed for this study are shown in the Appendix[17,18,28] (supplementary material).

The AMBER and MM2 force field equations are defined by equations I and II, respectively, in the Appendix (supplementary material). Among the differences between the two force field equations, MM2 uses cubic terms in the bond and angle contribution to the energy and employs a stretch-bend term. In MM2, 1,3-interactions are accounted for by the addition of this stretch-bend term. The

(25) The numbering systems for phenanthrene and biphenyl, respectively, are used.

(26) (a) Sanders, J. K. M.; Mersh, J. D. *Progr. NMR Spectrosc.* **1982**, *15*, 353–400. (b) Pirkle, W. H.; Pochapsky, T. C. *J. Am. Chem. Soc.* **1986**, *108*, 5627–5628.

(27) Allinger, N. L.; Gorden, B.; Profeta, S., Jr. *Tetrahedron* **1980**, *36*, 859–864.

(28) Beckhaus, H.-D. *Chem. Ber.* **1983**, *116*, 86–96.

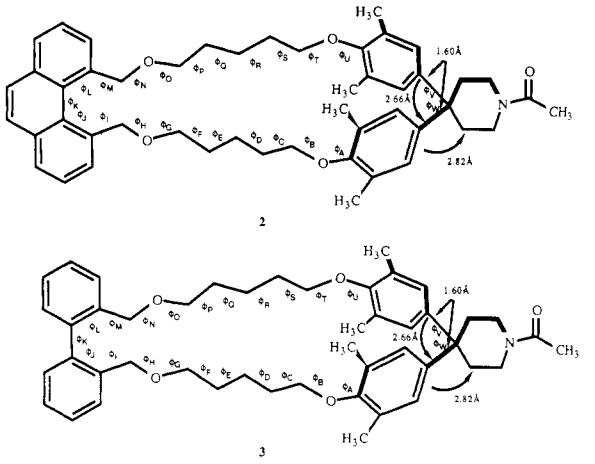

Figure 2. Distance constraints and dihedral angles used to generate the macrocyclic conformations with the ellipsoid algorithm.

MM2 force field describes the nonbonded interactions by the Hill equation,[29] while the AMBER force field uses a Lennard–Jones potential. Another difference between the force fields is that the electrostatic contribution in MM2 uses a Jeans' formula[30] in which the dipole–dipole interaction energy is the leading term. In AMBER a Coulombic potential is used to describe the electrostatic energy contribution. There have been several discussions of the differences between these two ways of evaluating electrostatic interactions.[17a,31]

Ellipsoid Algorithm and AMBER Force Field. The PREP, EDIT, and LINK routines of AMBER[18a] are designed to enable easy generation of complicated structures from small fragments. The initial structures of macrocyclic hosts **2** and **3** were derived by piecing together the two phenyl rings, the two ether side chains, the piperidine ring, and the phenanthrene moiety for **2** or the biphenyl moiety for **3**. The various parts were linked together, and the complete structure was optimized. The resulting conformation was the starting point used to generate 100 additional conformations of each macrocycle. The ellipsoid algorithm,[32a] which has been recently applied to the determination of polypeptide structure[32b] and docking studies of two flexible molecules,[32c] was used for this purpose. This algorithm uses torsional angles about single bonds as the degrees of freedom. Each conformation was obtained by randomly choosing a point in R^{n-1} conformational space, where n is the number of torsional angles along the macrocyclic ring. This program iteratively decreases the volume of an ellipsoid, defined by the resultant vectors of the torsional angles, by a constant value depending on n. If both van der Waals and distance constraints are not violated, an objective energy function is evaluated. This produces the smallest possible ellipsoid which asymptotically approaches a minimum. The selected variables for generation of conformations were 18 dihedral angles (ϕ_A–ϕ_I, ϕ_M–ϕ_U) of the macrocycle **2** and 19 dihedral angles (ϕ_A–ϕ_I, ϕ_K, ϕ_M–ϕ_U) of macrocycle **3** (Figure 2). Also the sp^2–sp^3 distance for the bonds to the tetrahedral carbon of the diphenylmethane unit was constrained to be less than 1.60 Å, the distance between the termini of the sp^2–sp^3–sp^2 angle of the diphenylmethane unit was constrained to be less than 2.66 Å, and the distance between one of these sp^2 carbons and a piperidine carbon atom adjacent to the tetrahedral center of the diphenylmethane unit was constrained to be less than 2.82 Å (Figure 2). These distance constraints were arbitrary upper bounds on the interatomic distances but were needed to ensure ring closure. The 1,3 distances imposed proper bond angles about the central diphenylmethane carbon atom in addition to defining a ring closure distance. Structures were formed by randomly generating dihedral angles (vide supra) for each conformation of the macrocycle and then refining the structure. Randomly generated dihedral angles were used to give an unbiased sampling of conformations.

Each structure generated in this way was minimized with the AMBER force field. For each calculation the energy was minimized with respect to all degrees of freedom by using analytical first derivatives. A constant dielectric of $\epsilon = 1.0$ was used. The calculation was terminated when the root-mean-square energy gradient was less than 0.05 kcal/Å or when the change in energy was less than 0.009 kcal/mol. The normal 1,4-electrostatic scaling factor EEL = 0.5 was used. Of the 100 conformations each of **2** and **3**, only 71 conformations of **2** and 86 of **3** converged to a total energy of less than 150 kcal/mol within 2600–5200 iterations of the AMBER force field. All of these remaining structures were then simulated for a total time of 5 ps (2500 steps) using molecular dynamics. The total simulation time of 5 ps was chosen in order to search the local regions of conformational space. Each simulation was carried out at an initial temperature of 1.2 K with a relaxation time of 0.1 ps to reach a final temperature of 300 K and constant pressure of 1 atm. In the molecular dynamics simulation the program assigns each atom of the molecule with small random velocities corresponding to 1.2 K. An initial set of positions, velocities, and values of the instantaneous forces are evaluated. The atoms are allowed to move in accord with Newton's equations of motion for a variable number of steps. Sets of successively greater random velocities are then assigned to the atoms, and they are allowed to move, until a temperature of 300 K is attained at 0.1 ps. A Gaussian distribution of this temperature is maintained for the duration of the simulation. The bond lengths were constrained with the SHAKE algorithm[33] during the molecular dynamics simulation. All of these structures were then reminimized with the AMBER force field. This procedure of minimizing to a local minimum, then using molecular dynamics to find a more stable minimum in that region of conformational space, and then reminimizing has been previously applied to 18-crown-6 ethers with some success in finding the low energy conformations,[34] although there are problems with locating high symmetry conformations.

MM2 Force Field. The coordinates of only 50 of the final conformations of macrocycles **2** and **3** generated in the AMBER force field study were used as initial geometries for the MM2 force field. Standard parameters were used whenever possible, but some new parameters had to be introduced for these calculations. The Beckhaus parameters were used for phenyl carbons.[28] The original force field does not have parameters for two sp^2-hybridized carbons which are formally singly bonded, such as present in biphenyl. A set of parameters (see Appendix) defining the 1–1′ bond of biphenyl was introduced which gave reasonable results for the known molecular structure of

(29) Hill, T. L. *J. Chem. Phys.* **1948**, *16*, 399–404.
(30) Lehn, J. M.; Ourisson, G. *Bull. Soc. Chim. Fr.* **1963**, 1113–1121.
(31) Boyd, D. B.; Lipkowitz, K. B. *J. Chem. Educ.* **1982**, *59*, 269–277.
(32) (a) Shor, N. Z. *Cybernetics* **1977**, *12*, 94–96. (b) Billeter, M.; Havel, T. F.; Wüthrich, K. *J. Comput. Chem.* **1987**, *8*, 132–141. (c) Billeter, M.; Havel, T. F.; Kuntz, I. D. *Biopolymers* **1987**, *26*, 777–793.
(33) Van Gunstern, W. F.; Berendsen, H. J. C. *Mol. Phys.* **1977**, *34*, 1311–1327.
(34) Billeter, M.; Howard, A. E.; Kuntz, I. D.; Kollman, P. A., submitted to *J. Am. Chem. Soc.*

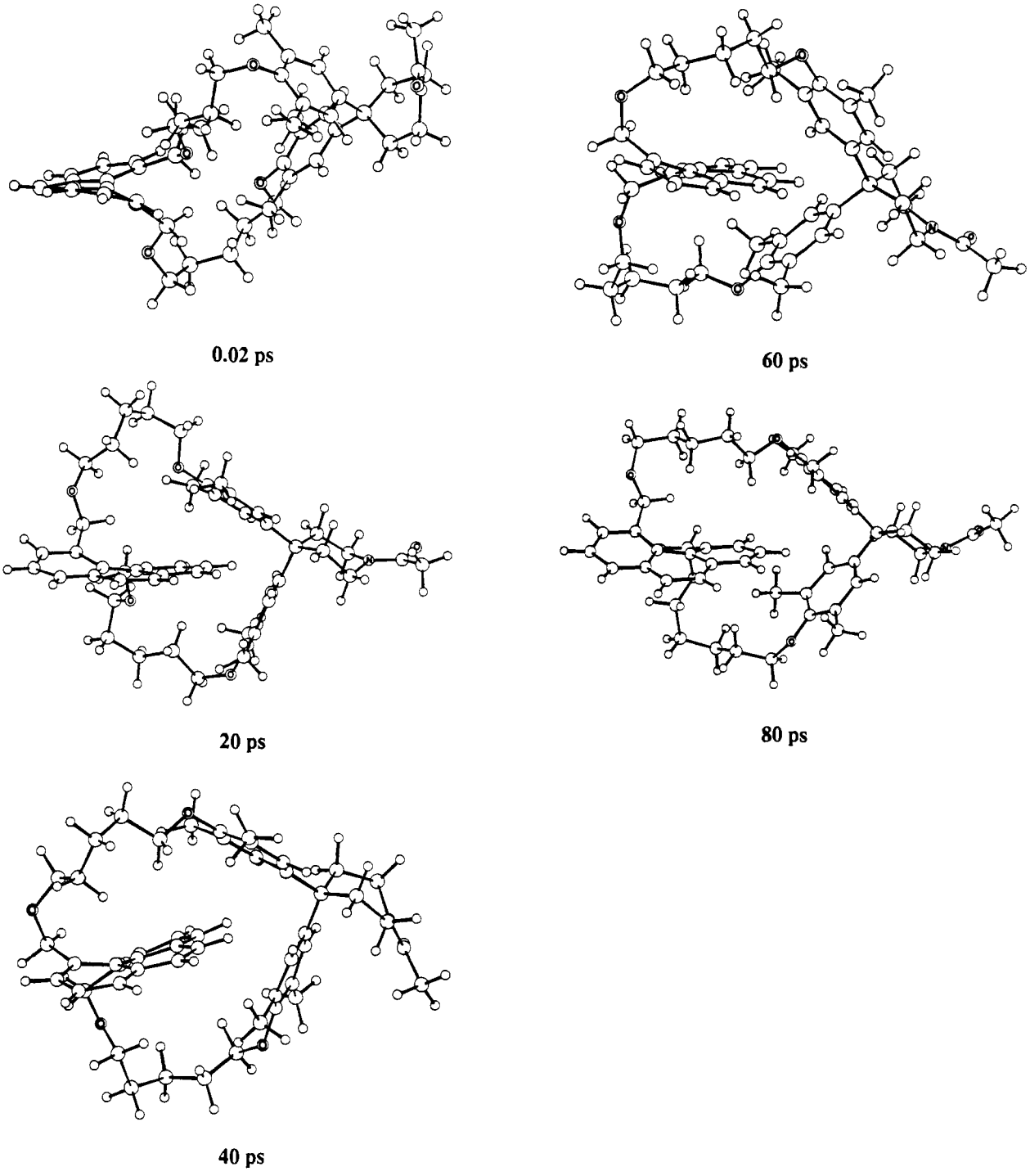

Figure 3. Several conformations of the 80-ps molecular dynamics simulations of the phenanthrene macrocycle **2**.

biphenyl[35] and a disubstituted biphenyl.[36b,c] The experimental[36a] torsional angle about the 1–1′ bond of biphenyl is 44–45°, whereas the calculated value is 45°.

Results

Molecular Dynamics Simulation. A molecular dynamics simulation was run on macrocycles **2** and **3** using 40 000 steps for a total simulation time of 80 ps. The calculation was conducted at constant pressure of 1 atm and temperature of 300 K. All bond lengths were constrained with the SHAKE algorithm.[33] Several conformations during the course of the simulation are shown in Figures 3 and 4. The initial conformation of each macrocycle shows the disubstituted aromatic moiety outside the molecular cavity. The simulation of macrocycle **2** rotated the phenanthrene moiety to a position about perpendicular to the mean plane of the macrocycle after 10 ps and then into the interior of the cavity at 40 ps. The phenanthrene moiety then hovers at the interior of the cavity for the duration of the simulation.

The molecular dynamics simulation of the biphenyl macrocycle **3** rotated one phenyl ring inside the cavity and then outside again. The flexible side chains cause the disubstituted biphenyl to rotate about the 1–1′ bond to

(35) Berlman, I. B. *Nature (London)* **1961**, *191*, 593–594.
(36) (a) Almenningen, A.; Bastiansen, O.; Fernholt, L.; Cyvin, B. N.; Cyvin, S. J. *J. Mol. Struct.* **1985**, *128*, 59–76. (b) Bastiansen, O.; Samdal, S. *J. Mol. Struct.* **1985**, *128*, 115–125. (c) Rømming, C.; Seip, H. M.; Aanesen Øymo, I.-M. *Acta Chem. Scand., Ser. A* **1974**, *28*, 507–514.

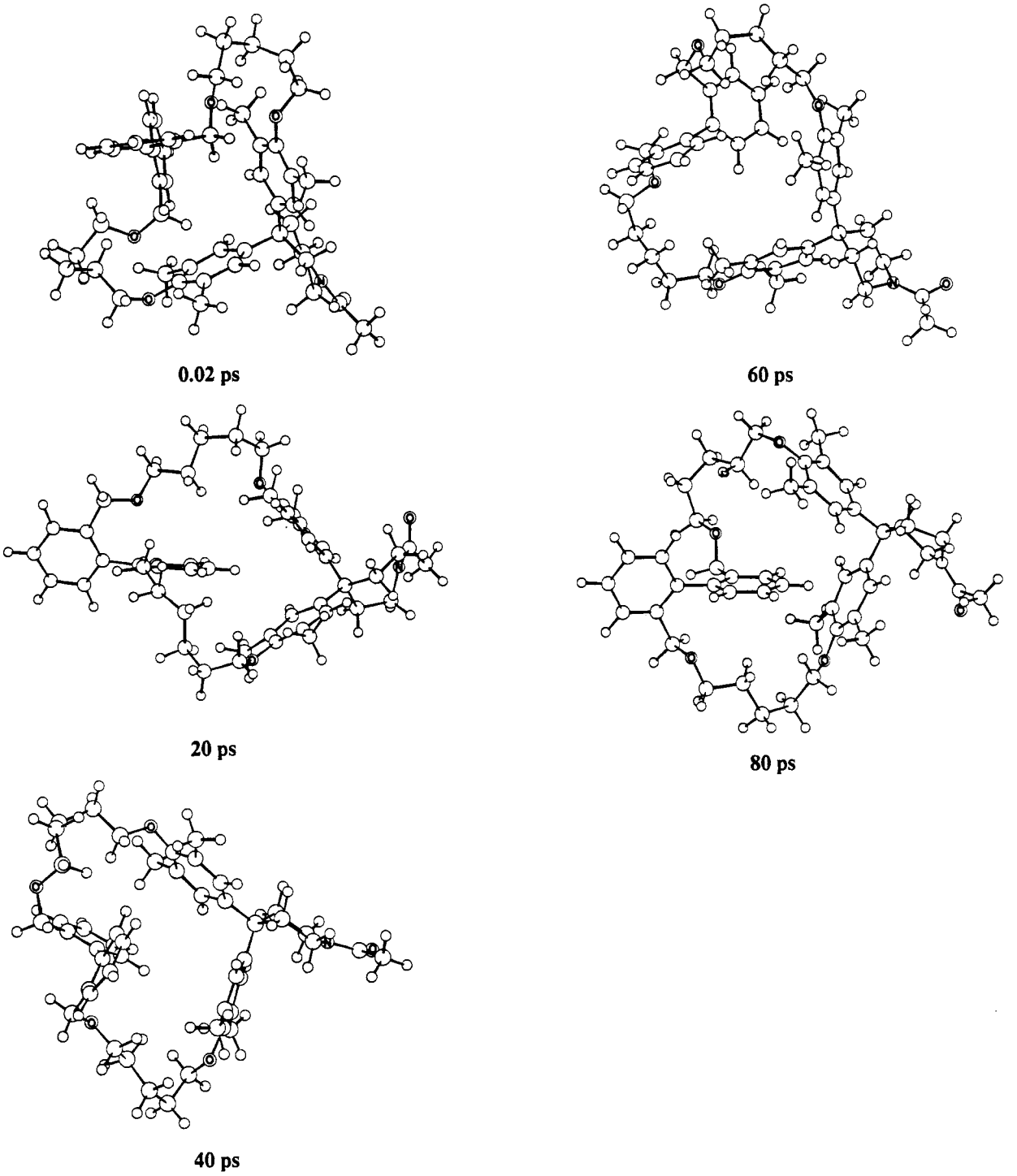

Figure 4. Several conformations of the 80-ps molecular dynamics simulation of the biphenyl macrocycle **3**.

a relatively high energy conformation. Without sufficient kinetic energy to overcome the barrier of rotation, estimated to be 16 kcal/mol,[37] one phenyl ring of the biphenyl turns inside the cavity, while the other phenyl ring remains outside. We refer to this orientation as the perpendicular conformation. The phenyl rings of the diphenylmethane unit provide assistance for the compression of one flexible side chain and for the stretching of the other side chain in order to allow this motion, giving a structure with the 1–1′ biphenyl axis pointing toward the diphenylmethane unit (20 ps). With the available kinetic energy at 300 K, the phenyl ring inside the cavity rotates outside the cavity, and the other phenyl ring moves into the cavity. A structure with the biphenyl completely filling the cavity results after 40 ps. The flexibility of the side chains enables the biphenyl moiety to move in dynamic equilibrium between conformations in the above fashion without ever overcoming the rotational barrier of the 1–1′ bond of the biphenyl moiety.

For both macrocycles **2** and **3**, the final geometry obtained after 80 ps of molecular dynamics simulation and subsequently being minimized by the AMBER force field technique was not the lowest energy conformation.

AMBER Force Field Optimizations. The results of the AMBER calculations are shown in Tables I and II. The calculations predict that the conformation **10-I**, with a total energy of 68.6 kcal/mol, is the lowest energy

(37) Eliel, E. L. *Stereochemistry of Carbon Compounds*; McGraw-Hill, Inc.: New York, 1962; p 177.

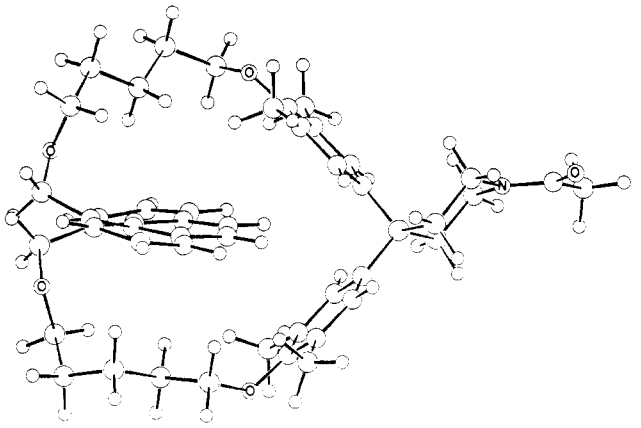

10-I

structure of the macrocycle **2** and is favored over all other conformations that were generated by the ellipsoid algorithm, subsequently minimized with the AMBER force field, simulated for 5 ps with molecular dynamics, and then reminimized (vide infra).

Structure **10-I** shows that the middle angle of the diphenylmethane unit is opened to 102.3°, giving an O···O distance of 8.34 Å for the O–Ar–C–Ar–O unit. The phenanthrene moiety is situated approximately in the center of the cavity. The short intramolecular distances of this conformation are shown in Table III. The C_{46}–C_{48} bond (9,10 bond) of the phenanthrene moiety is about 4.6 Å from the tetrahedral carbon of the diphenylmethane unit. However, the phenanthrene protons H_{47} and H_{49} (hydrogens on the 9,10 carbon atoms of phenanthrene) are as close as 2.65 Å to the carbon atoms of the aryl groups. The diphenylmethane spacer unit of **10-I** is characterized by the angles ϕ_V = 71.5° and ϕ_W = 76.6° between the least-squares planes of the two phenyl rings and the central plane defined by the atoms C_1–C_{95}–C_{87} (C_{sp^3}–C_{sp^2}–C_{sp^3}). This can be compared to the X-ray structure of diphenylmethane,[38] for which a helical form is found with angles ϕ_V = 63.9° and ϕ_W = 71.1° at −70 °C. The methylene groups attached to the phenanthrene moiety are 2.89 Å apart, which causes a large H_{35}···H_{61} interaction at a distance of only 2.03 Å. The torsional angle, ϕ_K, (C_{37}-$C_{45}C_{51}C_{58}$) of the phenanthrene moiety is −20°. This angle can be compared to the crystal structure of substituted phenanthrenes in which the dihedral between the A and C rings is generally between 20° and 35°.[39]

Structure **11-O** is the lowest energy conformation which has the phenanthrene moiety rotated completely outside of the molecular cavity. This structure is disfavored by 3.6 kcal/mol, mainly due to 0.4 kcal/mol of electrostatic interactions and 8.6 kcal/mol of less favorable van der Waals interactions, 4.4 kcal/mol of more favorable torsional strain energy, and 1.0 kcal/mol of more favorable bond and angle strain energy.

In **11-O**, the diphenylmethane unit angle is slightly larger at 106.8°, and the diphenylmethane unit differs from the geometry in **10-I**; this increases the O···O distance in the O–Ar–C–Ar–O unit to 9.23 Å. The diphenylmethane spacer unit of **11-O** is characterized by the angles ϕ_V = −86.5° and ϕ_W = −57.6°.

The structure **10-I** is favored over the perpendicular conformation, **12-⊥**, by 5.9 kcal/mol. The preference of

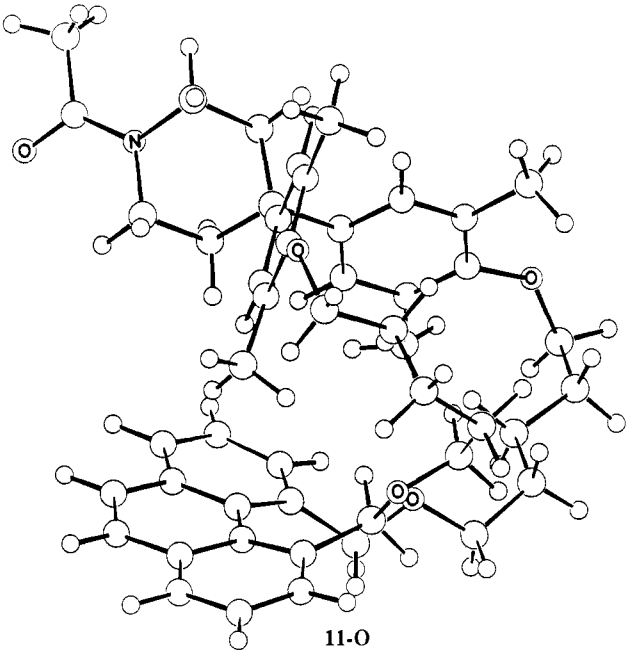

11-O

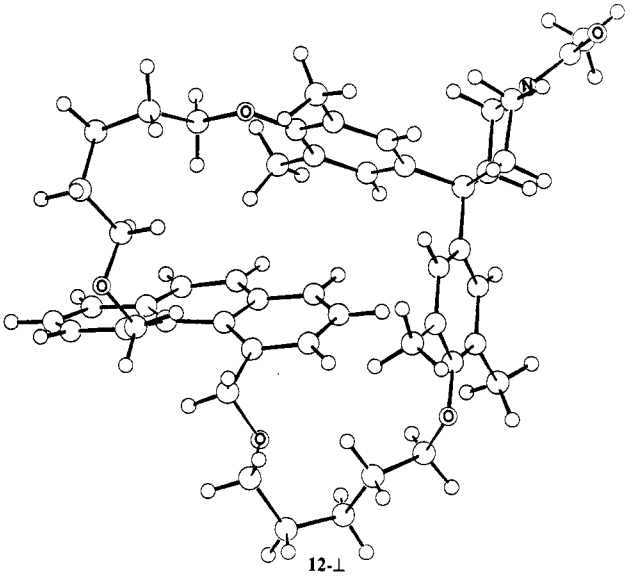

12-⊥

the inward conformation, **10-I**, is due to about 9.9 kcal/mol of more favorable van der Waals interactions and 1.1 kcal/mol of electrostatic interactions, while 5.1 kcal/mol of bond angle and torsional strain disfavor this conformation.

Structure **12-⊥** is twisted to a perpendicular conformation where one half of the phenanthrene moiety is rotated into the molecular cavity. The cavity of this structure appears to be somewhat larger than that found in **10-I**. The diphenylmethane unit angle is 105.5°, and the angles ϕ_V and ϕ_W are 69.2° and 71.5°, respectively.

The results obtained here by no means prove conclusively that the lowest energy conformation found here is indeed the global minimum, but such a large sampling of the possible conformations and the previous success of the ellipsoid algorithm combined with AMBER[34] suggest that it may very well be the global minimum. There are an estimated 5 million conformations[40] for this molecule due to the conformationally flexible connecting alkane side

(38) Barnes, J.; Paton, J.; Damewood, J., Jr.; Mislow, K. *J. Org. Chem.* **1981**, *46*, 4975–4979.

(39) (a) Saupe, T.; Krieger, C.; Staab, H. A. *Angew. Chem.* **1986**, *98*, 460–462; *Angew. Chem., Int. Ed. Engl.* **1986**, *25*, 451–453. (b) Cosmo, R.; Hambley, T. W.; Sternhell, S. *J. Org. Chem.* **1987**, *52*, 3119–3123.

(40) This number includes all possible conformations for an 18-unit alkyl chain where 14 dihedral angles have the 3 staggered arrangements 60°, −60°, 180° and 1 dihedral angle is fixed at a 0° conformation (i.e., 3^{14} = 4.783 × 10^6 conformations for 2,8,11,17-tetraoxaoctadecane).

Table I. Summary of Calculations on 30 Lowest Energy Conformations of Macrocycles 2 and 3[a]

macrocycle 2				macrocycle 3			
conf[b]	AMBER	conf	MM2	conf	AMBER	conf	MM2
10-I	0.0	**16-I**	0.0	**13-I**	0.0	**18-⊥**	0.0
11-O	3.6	**17-O**	5.7	**14-⊥**	1.7	**19-O**	2.0
I	4.4	O	6.6	I	2.2	**20-⊥**	2.0
12-⊥	5.9	O	6.8	I	2.8	**21-I**	2.2
⊥	8.1	⊥	6.9	⊥	2.9	O	2.3
O	9.4	⊥	8.4	⊥	3.2	⊥	2.9
O	9.5	⊥	8.6	⊥	3.3	O	2.9
O	11.3	O	8.7	**15-O**	4.4	⊥	3.0
O	11.9	O	9.0	⊥	4.7	O	3.2
I	12.2	O	9.1	O	4.9	O	3.5
	12.4		10.2		5.0		4.8
	12.5		11.1		5.2		4.9
	13.2		11.9		5.5		4.9
	13.3		12.0		5.6		5.2
	13.4		13.3		5.6		5.4
	13.6		13.9		6.2		5.8
	13.7		14.5		6.3		6.0
	13.8		14.7		6.3		6.0
	13.8		15.0		6.4		6.3
	14.0		15.2		6.6		6.9
	14.3		15.3		7.0		6.9
	14.3		15.6		7.3		7.1
	15.4		16.8		7.7		7.3
	15.5		17.2		7.8		7.4
	15.9		17.3		7.8		7.4
	15.9		17.4		8.1		8.2
	16.0		19.4		8.4		8.5
	16.5		20.2		8.7		8.6
	16.5		20.2		9.3		9.0
	17.6		20.5		9.3		9.1

[a] Energies are in kcal/mol. [b] The notations I, O, and ⊥ refer to the conformations inward, outward, and perpendicular.

Table II. Energetic and Geometric Results of Several Low Energy Conformations of Macrocycles 2 and 3 Calculated by the AMBER Force Field[a]

	macrocycle 2			macrocycle 3		
energy results	**10-I**	**11-O**	**12-⊥**	**13-I**	**14-⊥**	**15-O**
E_{rel}	0.0	3.6	5.9	0.0	1.7	4.4
E_T	68.6	72.2	74.5	33.8	35.5	38.1
el	0.0	0.4	1.1	1.2	0.5	0.5
VDW_{nb}	-13.9	-5.3	-4.0	-14.8	-11.8	-10.1
internal dihedral angles[b]	82.5	77.1	77.4	47.4	46.9	47.7
ϕ_A	-123	-139	-51	-11	-38	-57
ϕ_B	116	52	-116	-172	-159	-164
ϕ_C	178	177	177	53	-89	-81
ϕ_D	-168	165	-168	80	57	54
ϕ_E	-66	-63	58	-73	63	63
ϕ_F	-73	-45	40	-43	173	-178
ϕ_G	172	179	180	-72	175	82
ϕ_H	-79	-176	165	-176	179	-170
ϕ_I	-35	128	122	54	67	55
ϕ_J	-16	18	17	0	0	0
ϕ_K	-20	20	21	74	90	83
ϕ_L	-17	16	17	1	1	-1
ϕ_M	-35	-122	122	111	-177	52
ϕ_N	-78	-170	-76	-80	-174	-170
ϕ_O	168	170	172	171	70	171
ϕ_P	-70	-58	-172	-58	39	-173
ϕ_Q	-170	-170	-62	-55	52	172
ϕ_R	174	178	93	-57	-179	-90
ϕ_S	-68	89	-169	-170	172	76
ϕ_T	151	-72	160	-100	-70	-73
ϕ_U	-150	141	-167	125	-68	-56

[a] Energies are in kcal/mol. [b] See Figure 2 for the definition of the dihedral angles.

chains. The cavity-filling conformation of macrocycle **2** is lowest in energy because it has favorable van der Waals interactions and less torsional strain energy than other conformations.

Table III. Short Distances in Conformation 10-I (in Å)

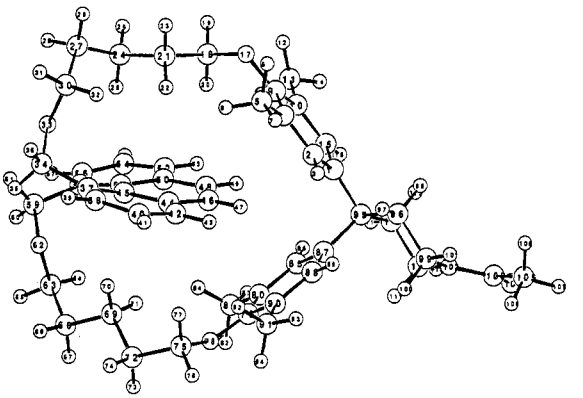

Aryl C(Phenanthrene)···C(Aryl) Distances			
C46···C1	3.80	C46···C2	3.47
C46···C4	3.43	C46···C9	3.72
C46···C80	3.33	C46···C79	3.49
C46···C85	3.44	C46···C87	3.72
C48···C9	3.59	C48···C10	3.56
C48···C15	3.72	C48···C80	3.50
C48···C85	3.49		
(Phenanthrene)···C(Aryl) Distances			
C1···H47	3.02	C2···H47	2.65
C4···H47	2.97	C79···H47	3.10
C80···H47	3.04	C85···H47	2.89
C87···H47	2.83	C88···H47	2.91
C90···H47	3.06	C10···H49	2.90
C15···H49	2.87	C85···H49	2.98
Other Short Distances			
H3···H47	2.82	O33···C58	2.95
O33···C51	3.08	H35···H61	2.03
C37···C59	3.28	C44···H70	2.99
C45···O62	3.09	H49···H86	2.73
H57···H60	2.20	C58···H64	2.69

As mentioned previously, the macrocycle **3** was originally studied in order to determine whether it was possible to predict whether the inward or outward conformation was preferred. Force field calculations of only three arbitrary conformations of macrocycle **3** suggested that the outward conformation was tentatively preferred by about 2 kcal/mol. After these initial predictions, a more rigorous conformational analysis, using the ellipsoid algorithm, was employed to study the conformational behavior of macrocycle **3** and is now discussed below.

The AMBER force field calculations predict that conformation **13-I**, which has the biphenyl moiety inside the cavity, is lowest in energy. The energetics and torsion

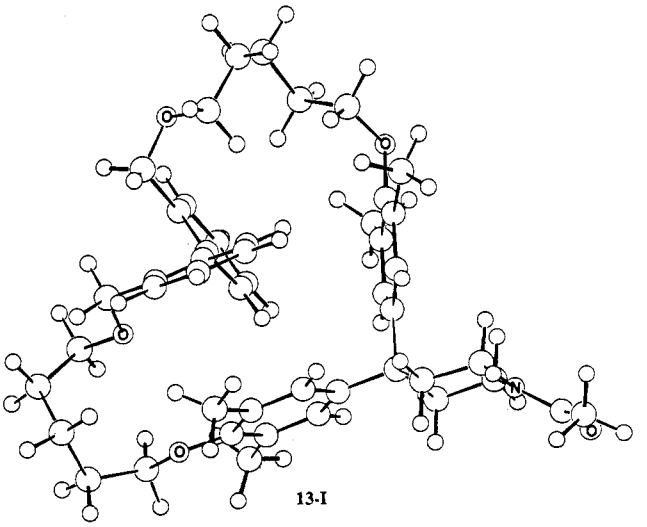

13-I

Table IV. Short Distances in Conformation 13-I (in Å)

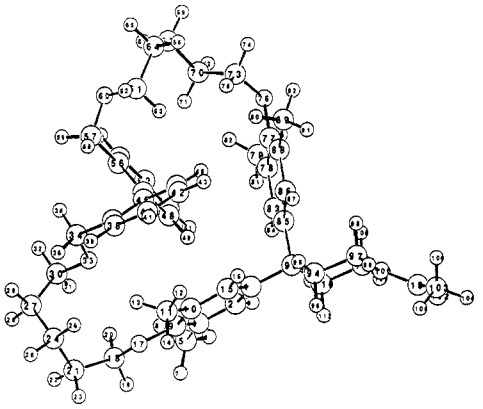

Aryl C(Biphenyl)···C(Aryl) Distances			
C44···C15	3.88	C44···C86	3.80
C44···C88	3.86	C48···C1	3.87
C48···C10	3.87	C48···C2	3.72
C48···C4	3.74	C48···C15	3.99
C48···C78	3.73	C48···C83	3.57
C50···C78	3.66	C50···C83	3.69
(Biphenyl)H···C(Aryl) Distances			
H45···C86	2.97	H45···C88	2.83
H49···C1	2.82	H49···C2	2.77
H49···C4	2.91	H49···C9	3.07
H49···C10	3.08	H49···C15	2.95
H49···C83	3.16		
Other Short Distances			
H13···C37	2.92	O33···C47	2.92
H35···H58	2.32	H36···H39	2.32
C37···H58	2.73	C46···H58	2.61
C56···H63	2.71		

angles along the flexible chains are also shown in Table II. The planes formed by the phenyl rings of the biphenyl unit are nearly perpendicular (74°). For macrocycle **3** the lowest energy conformation has a slightly larger cavity opening than the lowest conformation of macrocycle **2** (**10-I**). The bond angle about the tetrahedral carbon of the diphenylmethane spacer unit is 105.8°. The O···O distance of O–Ar–C–Ar–O is 9.23 Å, as compared to 8.34 Å for **10-I**. Short distances of conformation **13-I** are shown in Table IV. Noticeably the Aryl C(biphenyl)···C(Aryl) and (biphenyl)H···C(Aryl) distances appear to be larger than the Aryl C(phenanthrene)···C(Aryl) and (phenanthrene)H···(Aryl)C distances of **10-I** shown in Table III.

Structure **14-⊥** is 1.7 kcal/mol higher in energy than **13-I**. This structure has one phenyl ring of the biphenyl moiety completely inside of the cavity and the other phenyl ring outside of the cavity. Structure **14-⊥** is disfavored

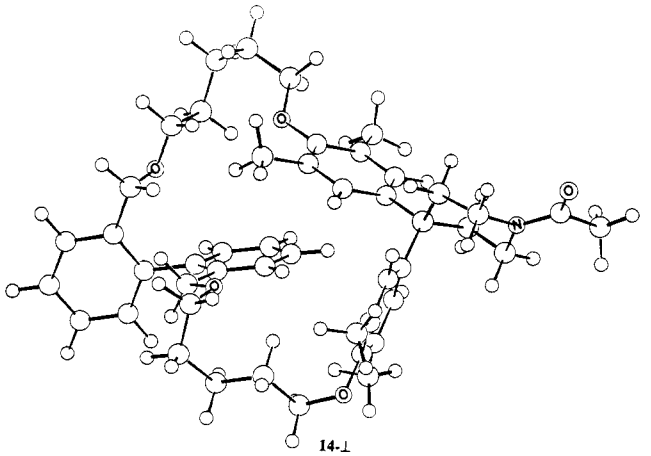

14-⊥

by 1.7 kcal/mol due to 3.0 kcal/mol less favorable van der Waals interactions, 0.7 kcal/mol more favorable electrostatic interactions, and 0.5 kcal/mol more favorable internal energy contributions. Table V shows the short contact distances of **14-⊥**. These can be compared to the short contact distances for **10-I**. The (biphenyl)H···C(Aryl) distances appear to be much larger than those of **10-I** shown in Table III, which is in accord with the induced chemical shift observations in the NMR studies. The bond angle about the tetrahedral carbon of the diphenylmethane spacer unit of **14-⊥** is 106.2°. The O···O distance of the O–Ar–C–Ar–O unit is a large value of 9.24 Å.

Table V. Short Distances in 14-⊥ (in Å)

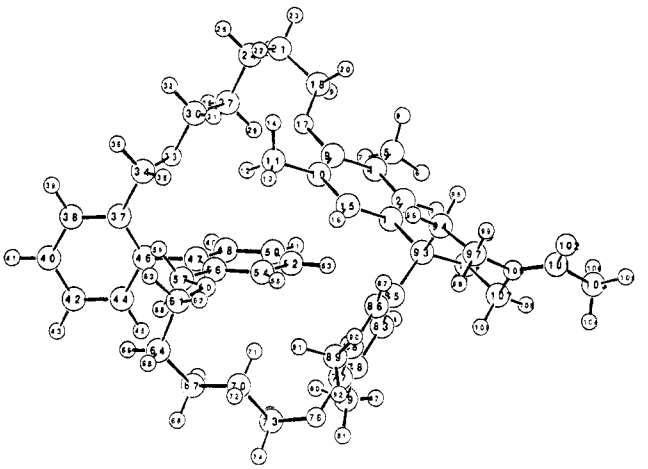

Aryl C(Biphenyl)···C(Aryl) Distances			
C50···C9	3.89	C52···C1	3.90
C52···C2	3.88	C52···C4	3.66
C52···C9	3.42	C52···C10	3.40
C52···C15	3.65	C54···C10	3.41
C54···C15	3.59		
(Biphenyl)H···C(Aryl) Distances			
H53···C1	3.11	H53···C2	3.02
H53···C4	3.08	H53···C9	3.23
H53···C10	3.27	H53···C15	3.22
H53···C83	3.21	H55···C10	3.28
H55···C15	3.08	H55···C83	3.35
Other Short Distances			
H35···H59	2.45	H49···O33	3.04
H53···H84	2.73	C54···H12	3.10

Structure **15-O** is the lowest energy conformer which has the biphenyl moiety outside the cavity. This conformer is 4.4 kcal/mol higher in energy than structure **13-I**.

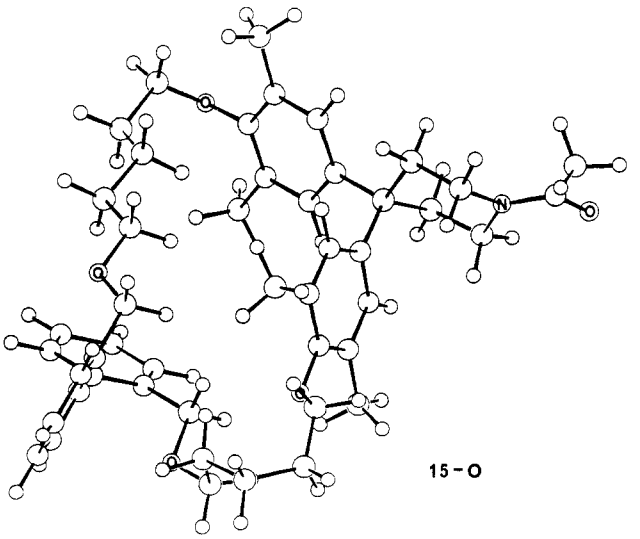

15-O

A Boltzmann distribution was performed on the 10 lowest conformations for the AMBER calculations of

Table VI. Energetic and Geometric Results of Several Low Energy Conformations of Macrocycles 2 and 3 Calculated by Using the MM2 Force Field[a]

	macrocycle 2		macrocycle 3			
energy results	**16-I**	**17-O**	**18-⊥**	**19-O**	**20-⊥**	**21-I**
E_{rel}	0.0	5.7	0.0	2.0	2.0	2.2
E_T	80.9	86.6	44.1	46.1	46.1	46.3
el	0.1	1.0	-0.1	0.3	0.4	0.5
VDW_{nb}	-22.1	-18.2	-23.6	-20.8	-20.9	-24.9
internal dihedral angles[b]	102.8	103.9	67.8	66.5	66.5	70.7
ϕ_A	-113	-100	-97	-84	-80	-75
ϕ_B	113	-172	-175	-164	-166	-166
ϕ_C	174	59	169	-69	-65	73
ϕ_D	-168	71	68	61	65	93
ϕ_E	-65	-172	-167	57	52	-60
ϕ_F	-74	70	66	-175	180	-53
ϕ_G	171	-179	92	85	171	-78
ϕ_H	-81	70	-77	-172	179	-179
ϕ_I	-30	30	118	50	68	47
ϕ_J	-18	22	-1	0	-1	1
ϕ_K	-22	27	90	81	90	73
ϕ_L	-20	21	2	0	-1	1
ϕ_M	-32	-135	-53	46	-177	115
ϕ_N	-81	-178	179	-174	-175	-79
ϕ_O	164	65	-166	173	72	164
ϕ_P	-72	50	173	-179	38	-63
ϕ_Q	-174	174	-169	174	52	-58
ϕ_R	176	-78	69	-179	-178	-54
ϕ_S	-75	-91	63	84	172	-162
ϕ_T	144	57	-163	-69	-65	-85
ϕ_U	-132	76	104	-75	-77	110

[a] Energies are in kcal/mol. [b] See Figure 2 for the definition of the dihedral angles.

macrocycle **3**. Only the conformations classified as out (O) and in (I) were included in the Boltzmann distribution. The calculation predicts an inward:outward ratio of 99:1. This macrocycle is predicted to exist in the inward conformation all of the time by these calculations.

It should be noted that the AMBER aromatic torsional parameters[19c] were varied to investigate if the qualitative results were dependent on the exact parameters. A much softer $V_{n/2}$ term of 9.2, instead of the 30.0, was used for the torsional parameters (see Appendix; supplementary material). The qualitative results of force field calculations on phenanthrene macrocycle **2** did not change. The calculations with softer torsional parameters predicted that the inward conformation, **10-I'**, was favored by 6.5 kcal/

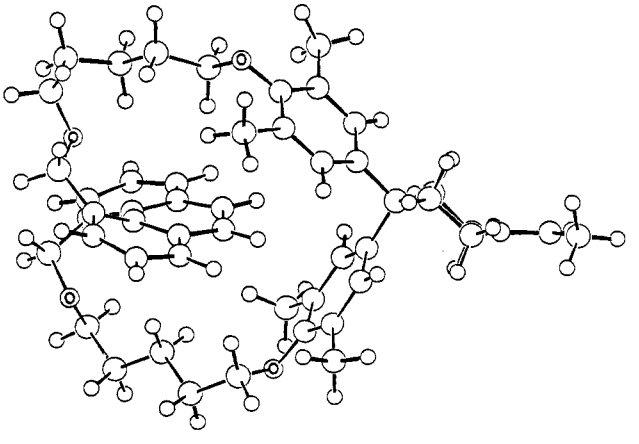

10-I'

mol over the outside conformation. The resulting geometries of these calculations showed a dihedral angle (33°) between the A and C rings of phenanthrene, ϕ_K, which was closer to the corresponding value (33°) in the crystal structure of 4,5-dimethylphenanthrene.[39b] However in a few of the conformations, the para-substituted phenyl rings of the diphenylmethane unit would distort 10–20° away from planarity. The calculations of the biphenyl macrocycle **3**, with softer aromatic parameters, predicted a preference for the perpendicular conformation by 0.9 kcal/mol over the inside conformation.

MM2 Force Field Optimizations. The results of the MM2 force field calculations are presented in Table VI. The MM2 force field also predicts that the phenanthrene moiety of macrocycle **2** is favored inside of the molecular cavity. The structure **16-I** is favored by 5.7 kcal/mol over

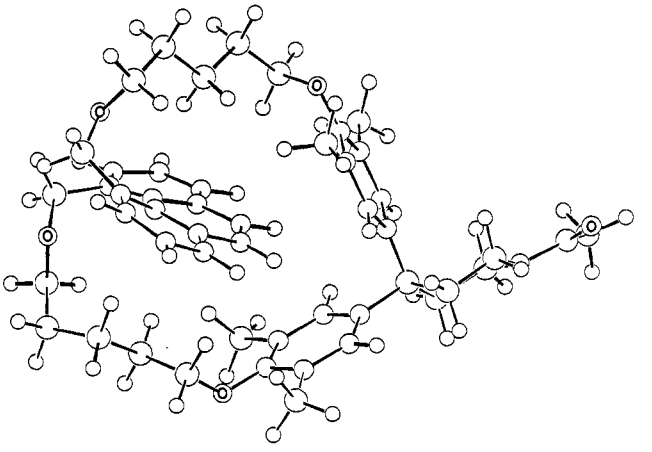

16-I

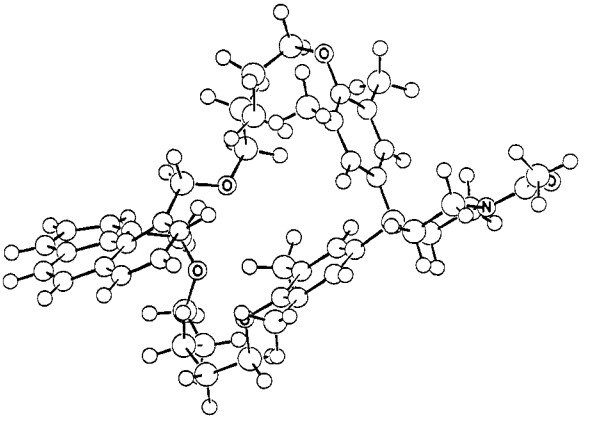

17-O

conformation **17-O** with the phenanthrene moiety outside the cavity. The preference of inward conformation is 2.1 kcal/mol greater than that predicted by the AMBER force field calculations. The major factor contributing to the preference of conformation **16-I** over **17-O** is again the more favorable van der Waals interactions in **16-I**. Structure **16-I** is similar to the AMBER structure **10-I**. The O···O distance of the O–Ar–C–Ar–O unit is 8.58 Å. A most obvious difference between these two structures is the carbon–carbon interaction of the methylene units attached to the phenanthrene moiety. In **16-I**, the $C_{34}\cdots C_{59}$ distance is 3.01 Å, and the $H_{35}\cdots H_{61}$ distance is 1.98 Å, whereas these distances are 2.89 and 2.03 Å, respectively, in **10-I**. With -20° in **10-I** and -22° in **16-I**, the torsional angles, ϕ_K, ($C_{37}C_{45}C_{51}C_{58}$) of the phenanthrene units are very similar.

The lowest energy conformation of macrocycle **3** is predicted by MM2 to have one ring of the biphenyl moiety rotated inside the molecular cavity. This structure **18-⊥**

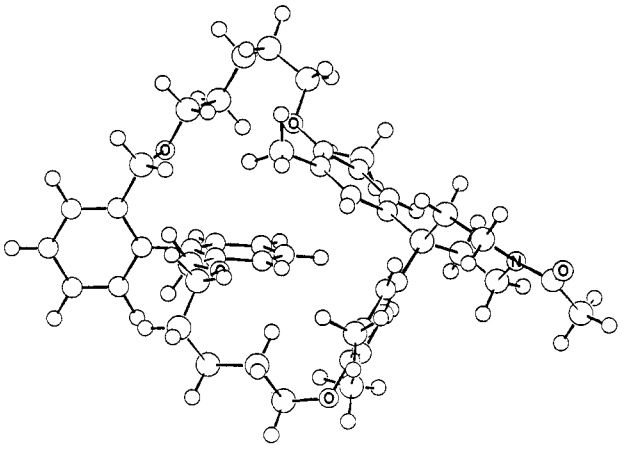

18-⊥

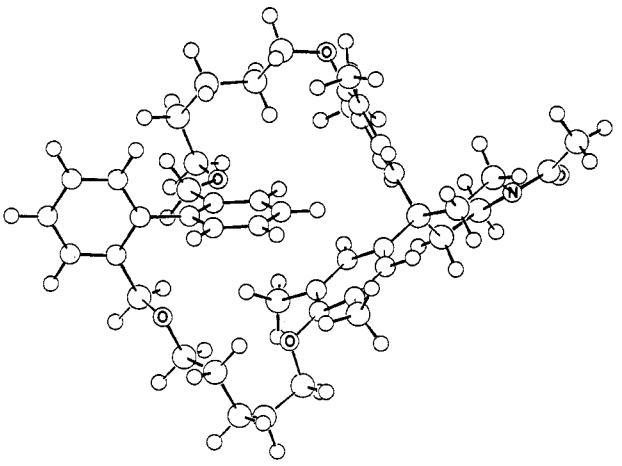

20-⊥

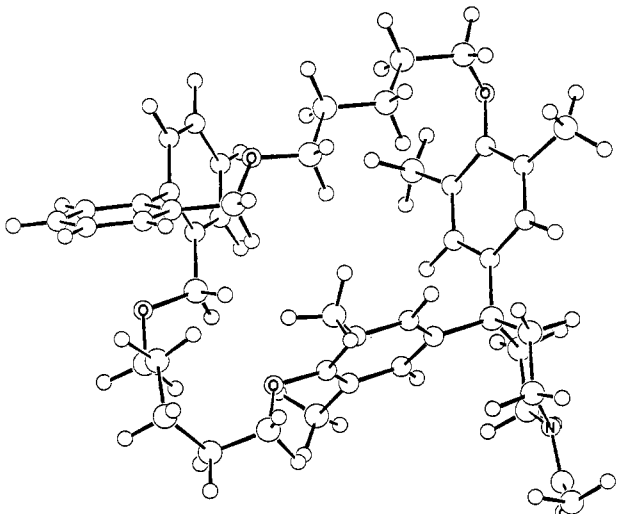

19-O

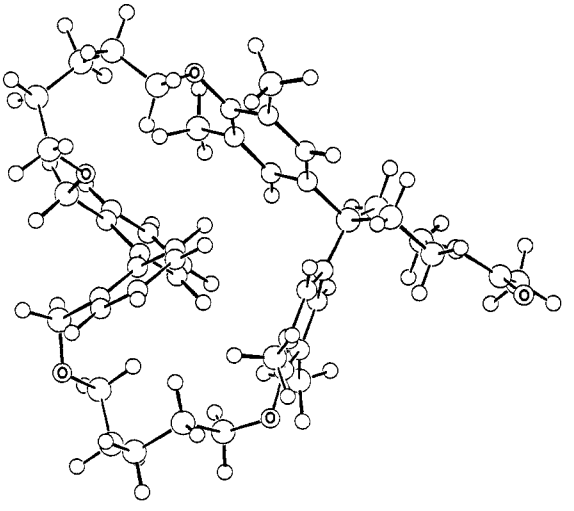

21-I

is favored over structure **19-O** by 2.0 kcal/mol. The preference again occurs because of favorable van der Waals interactions. In structure **19-O** with the biphenyl moiety completely outside the cavity, the angle about the tetrahedral carbon of the diphenyl spacer unit is 107.3°. The O···O distance of the O–Ar–C–Ar–O unit is large at a value of 9.32 Å. Structure **20-⊥** has about 7 gauche butane type interactions, yet is only 2.0 kcal/mol higher in energy than **18-⊥**. Structure **21-I** has 1.3 kcal/mol more favorable van der Waals interactions than **18-⊥** but 2.9 kcal/mol less favorable internal energy contributions.

A Boltzmann distribution over the 10 lowest energy conformations of macrocycle **3** using the MM2 force field predicts a 26:74 ratio of inward to outward conformations. A much larger preference for the outward conformations is seen here than with the AMBER force field calculations. The results here are much closer to the experimental results.

The overall results of the conformational analysis using both force fields are quite similar for the phenanthrene macrocycle **2**, but differ to a greater extent for the biphenyl macrocycle **3** (Table I). Both AMBER and MM2 predict the preferred conformation of macrocycle **2** to contain the phenanthrene moiety inside the cavity. This conformation is preferred over the outward conformation by 4–6 kcal/mol. The AMBER force field predicts that the lowest energy conformation of macrocycle **3** is the inside conformation. This force field predicts a greater preference for the inside and perpendicular conformations than for the outside conformation. In the perpendicular conformation one phenyl ring is approximately inside the cavity while the other ring is outside the cavity. The MM2 force field also predicts a preference for the perpendicular form. The perpendicular form is lower in energy than the inside conformation by about 2 kcal/mol. The major difference in the results of the two force fields is the relative energies of the full inward and outward conformations. With AMBER the inward conformation is favored over the outward conformation by 4.4 kcal/mol. With MM2 the outward conformation is lower in energy than the inward conformation by a small value. These differences are a result of the differences in the two force fields.

Conclusion. In agreement with the experimental results, both AMBER and MM2 force field calculations indicate that the phenanthrene macrocycle **2** prefers the inward conformation by 4–6 kcal/mol due to very favorable van der Waals interactions with the interior of the cavity. The apolar phenanthrene unit is better stabilized by the apolar interior of the cavity. This preference should be even greater in polar solvents. Both force fields also support the relevance of cavity-filling conformations for the biphenyl macrocycle **3**. The MM2 calculations show a larger preference than AMBER calculations for the perpendicular conformation of **3** with one phenyl ring of the biphenyl moiety folded inside the cavity and therefore seem to be in better agreement with the experimental results. Both force field calculations suggest that favorable van der Waals interactions within the interior of the cavity lead to a preference of inside over outside conformations. The described molecular modeling studies completely neglect the dependence of macrocycle conformation on

solvation enthalpy and entropy. Therefore, the good agreement between experimental results obtained in solution and gas-phase force field calculations seen in this work is noteworthy.

Experimental Section

Instrumentation and Analytical Methods. ^{1}H NMR spectroscopy was carried out at 303 K on Bruker WP200, HX 360, and AM 500 spectrometers. All δ values (ppm) refer to Me_4Si as internal standard. Mass spectra were carried out on a AEI MS9 spectrometer and a AEI MS902 high resolution mass spectrometer. EI mass spectra were recorded at 70 eV. Melting points (uncorrected) were measured on a Büchi (Dr. Tottoli) apparatus. IR spectra were recorded on a Perkin-Elmer PE580 instrument. Elemental analysis was performed at Spang Microanalytical Laboratory, Eagle Harbor, MI. Solvents and reagents were purchased from Aldrich Chemical Company and were used without further purification unless otherwise specified.

2D NOESY ^{1}H NMR. The 500-MHz 2D NOESY spectra of **2** or **3** were obtained by using the Bruker version 850101 software which incorporates a 90°–t_1–45°–t_m–45° pulse sequence (t_m = mixing time). The sweep width along F1 was 3760 Hz and along F2 was 1880 Hz with a matrix size of 256 × 1024 data points. The 256 incremental spectra were recorded by a sequence involving 2 dummy scans and 4 accumulations. The relaxation delay was 2 s and the initial mixing time was 1 s, which was varied ±2%. The data matrix was completed by zero-filling in F1 to give 512 data points. The FID data were processed by a sine bell window function followed by Fourier transformation. The matrix was symmetrized to suppress signals that cannot be correlated. The digital resolution was 7.3 Hz/point.

The COSY spectra were recorded by using the 90°–t_1–90° pulse sequence and treated in a similar way as described for the NOESY spectra.

Syntheses. 2,2′-Bis[(5-chloropentoxy)methyl]biphenyl (5). A total of 6.4 g (0.04 mol) of potassium hydride (25% dispersion in oil) was washed with 3 × 20 mL portions of dry hexane under an argon atmosphere. It was then suspended in 50 mL of tetrahydrofuran and dried over sodium, and a catalytic amount of 18-crown-6 was added. To the stirred suspension was added 2.14 g (0.01 mol) of 2,2′-bis(hydroxymethyl)biphenyl[22] in portions. After the hydrogen evolution had ceased, 12 mL (0.1 mol) of 1,5-dichloropentane, dried over basic alumina, was added dropwise to the reaction mixture. After heating to reflux for 2 h, thin layer chromatography (SiO_2, EtOAc) indicated the completion of the reaction. The mixture was cooled and the excess of potassium hydride was destroyed by dropwise addition of methanol. The solvents were removed under reduced pressure and the residue was distributed between dichloromethane and water. The organic layer was washed with 4 portions of water followed by saturated NaCl and dried over magnesium sulfate. The solvent was distilled off, leaving a pale yellow oil. Chromatography on silica gel from *n*-hexane to remove the excess of 1,5-dichloropentane and finally from *n*-hexane/dichloromethane (1:1) afforded 3.0 g (71%) of the dichloride **5** as a colorless oil: IR (film) ν(C–H) 2900, 2700 cm^{-1}; ^{1}H NMR (500 MHz, 1D and 2D COSY, $CDCl_3$) δ 1.43 (mc, 4 H, $OCH_2CH_2CH_2$),[41] 1.51 (mc, 4 H, OCH_2CH_2), 1.72 (mc, 4 H, CH_2CH_2Cl), 3.28 (t, J = 6.4 Hz, 4 H, $ArCH_2OCH_2$), 3.48 (t, J = 6.7 Hz, 4 H, CH_2Cl), 4.18 (s, 4 H, $ArCH_2O$), 7.14 (dd, J = 7.5 and 1.3 Hz, 2 H, 6,6′-H), 7.29 (dt, J = 7.5 and 1.3 Hz, 2 H, 5,5′-H), 7.37 (dt, J = 7.5 and 1.3 Hz, 2 H, 4,4′-H), 7.53 (dd, J = 7.5 and 1.3 Hz, 2 H, 3,3′-H); MS, m/z (relative intensity) 300 (41, M^+ – H – $O(CH_2)_5Cl$), 179 (100, M^+ – H –2[$O(CH_2)_5Cl$]); HRMS, m/z (M^+ – H – $O(CH_2)_5Cl$) calcd 300.1281, obsd 300.1293, m/z (M^+ – H – 2[$O(CH_2)_5Cl$]) calcd 179.0861, obsd 179.0851.

1′-Acetyl-30,34,38,40-tetramethylspiro[1,7,22,28-tetraoxa-[8](2,2′)biphenyleno[8.1]paracyclophane-35,4′-piperidine] (3). A total of 2.53 g (6.0 mmol) of **5**, 2.20 g (6.0 mmol) of 1-acetyl-4,4-bis(4-hydroxy-3,5-dimethylphenyl)piperidine (**6**), and 6.4 g (0.02 mol) of cesium carbonate in 300 mL of dimethylacetamide, dried over potassium carbonate, was stirred at 90 °C under nitrogen for 4 days. After cooling, the inorganic salts were removed by filtration through a bed of Celite. The solvent was evaporated under reduced pressure and the residue was chromatographed on silica gel from dichloromethane followed by ethyl acetate/dichloromethane (2:5) to give 860 mg (21%) of **3** as a colorless glass. A microanalytically pure sample was obtained after a second chromatography on silica gel from ethyl acetate/dichloromethane (1:5): IR (KBr) ν(C=O) 1625 cm^{-1}; ^{1}H NMR (500 MHz, 1D and 2D COSY, $CDCl_3$) δ 1.30 (mc, 4 H, $OCH_2CH_2CH_2$), 1.41 (mc, 4 H, $CH_2OCH_2CH_2$), 1.65 (mc, 4 H, CH_2CH_2OAr), 2.08 (s, 3 H, CH_3CON), 2.17 (s, 12 H, Aryl-CH_3), ~2.29 (mc, 4 H, CH_2CH_2N), 3.22 (mc, 4 H, $ArCH_2OCH_2$), ~3.52 (mc, 4 H, CH_2CH_2N), 3.70 (mc, 4 H, CH_2OAr), 4.04 and 4.12 (AB, J_{AB} = 12.0 Hz, 4 H, $ArCH_2O$), 6.83 (s, 4 H, Ar-$H_{diphenmeth}$), 7.04 (m, 2 H, 6,6′-$H_{biphenyl}$), 7.10 (mc, 4 H, 4,4′-H and 5,5′-H), 7.38 (m, 2 H, 3.3′-H); MS, m/z 717 (M^+). Anal. Calcd for $C_{47}H_{59}NO_5$ (717.9): C, 78.66; H, 8.23; N, 1.95. Found: C, 78.60; H, 8.25; N, 1.84.

Acknowledgment. This work was supported by grants from the National Science Foundation (CHE-8617409 to F.D.) and CHE-8512785 to K.N.H.) and a generous grant of computer time from the NSF-sponsored San Diego Supercomputer Center. We acknowledge the support for the purchase of the Silicon Graphics IRIS 3130 workstation provided by the Office of Naval Research and by a National Institutes of Health Biomedical Research Support Grant. R.J.L. and F.K.B. would like to thank Martin Billeter for the use of the ELLIPSE program and Allison E. Howard for her assistance in its use. R.J.L. would also like to thank Peter A. Kollman for his helpful discussions and the use of the UCSF Computer Graphics Lab. The structures presented in this manuscript were prepared with a Macintosh drawing program developed by Michael D. Miller at Los Angeles.

Supplementary Material Available: Equations describing the AMBER and MM2 force fields, additional AMBER and MM2 parameters, and the net atomic charges for the fragments of macrocycles **2** and **3** used in the AMBER minimization (6 pages). Ordering information is given on any current masthead page.

(41) The multiplet centers are used to calculate the cyclization shifts shown in Figure 1.